

## Article

# Sandaracinobacteroides saxicola sp. nov., a Zeaxanthin-Producing and Halo-Sensitive Bacterium Isolated from Fully Weathered Granitic Soil, and the Diversity of Its ARHDs

Ying Tang \*, Cuiyang Zhang, Qingshan Long, Ping Lei, Zhaohui Guo \* and Qingshu Liu \*

Hunan Institute of Microbiology, Changsha 410009, China

\* Correspondence: tangying@hnwyy.cn (Y.T.); guozhaohui@hnwyy.cn (Z.G.); qingshu\_liu@sina.com (Q.L.)

**Abstract:** A yellow, Gram-stain-negative, aerobic, non-spore-forming, motile, and rod-shaped bacterial strain designated M6<sup>T</sup> was isolated from fully weathered granitic soil. The strain showing the highest 16S rRNA gene sequence similarity to M6<sup>T</sup> was *Sandaracinobacteroides hominis* SZY PN-1<sup>T</sup> (96.3%), the only species in the genus *Sandaracinobacteroides*. The average nucleotide identity and digital DNA-DNA hybridization value between these two strains were 72.6% and 18.0% respectively. Growth was inhibited by NaCl ( $\geq 0.1\%$  (*w/v*)). Strain M6<sup>T</sup> contained C<sub>18:1</sub> $\omega$ 7c (33.8%), C<sub>14:0</sub> 2-OH (16.6%), summed feature 3 (15.8%), and C<sub>16:0</sub> (12.6%) as the major fatty acids. The polar lipids profile consisted of phosphatidylglycerol, phosphatidylethanolamine, an unidentified glycolipid, four unidentified phospholipids, and four unidentified lipids. The genome of strain M6<sup>T</sup> was 3.4 Mb with 67.7% GC content. Further genomic analysis revealed a biosynthetic gene cluster for zeaxanthin, the production of which was verified by a high-resolution mass spectrum. The existence of multiple genes for aromatic ring-hydroxylating dioxygenases implies the potential ability for organic pollution controlling. The morphological, physiological, chemotaxonomic, and phylogenetic analysis clearly distinguished this strain from its phylogenetic neighbors, thus strain M6<sup>T</sup> represents a novel species of the genus *Sandaracinobacteroides*, for which the name *Sandaracinobacteroides saxicola* sp. nov. is proposed. The type of strain is M6<sup>T</sup> (=CGMCC 1.19164<sup>T</sup>=NBRC 115420<sup>T</sup>).

**Keywords:** novel species; *Sandaracinobacteroides saxicola*; whole genome sequence; zeaxanthin; aromatic ring-hydroxylating dioxygenase; biodegradation



**Citation:** Tang, Y.; Zhang, C.; Long, Q.; Lei, P.; Guo, Z.; Liu, Q. *Sandaracinobacteroides saxicola* sp. nov., a Zeaxanthin-Producing and Halo-Sensitive Bacterium Isolated from Fully Weathered Granitic Soil, and the Diversity of Its ARHDs. *Diversity* **2022**, *14*, 807. <https://doi.org/10.3390/d14100807>

Academic Editor: José Luis García-Marín

Received: 10 August 2022  
Accepted: 22 September 2022  
Published: 27 September 2022

**Publisher's Note:** MDPI stays neutral with regard to jurisdictional claims in published maps and institutional affiliations.



**Copyright:** © 2022 by the authors. Licensee MDPI, Basel, Switzerland. This article is an open access article distributed under the terms and conditions of the Creative Commons Attribution (CC BY) license (<https://creativecommons.org/licenses/by/4.0/>).

## 1. Introduction

The genus *Sandaracinobacteroides*, a member of the family *Sphingosinellaceae*, order *Sphingomonadales*, and class *Alphaproteobacteria* was proposed in 2021 [1]. A similar genus *Sandaracinobacter* with closely phylogenetic distance had been described in 1997 [2], and subsequently amended in 2020 [3], however, this genus is not a validly published name according to the List of Prokaryotic Names with Standing in Nomenclature ([www.bacterio.net](http://www.bacterio.net) (accessed on 19 July 2022)) [4].

At the time of writing, the genus *Sandaracinobacteroides* includes only one species, the *S. hominis* SZY PN-1<sup>T</sup> originated from human skin [1]. The genus *Sandaracinobacter* contains 2 species, the *S. sibiricus* RB16-17<sup>T</sup> and *S. neustonicus* PAMC 28131<sup>T</sup>. They originated from freshwater and sea surface microlayers respectively [2,3]. All three species were Gram-stain-negative, strictly aerobic, or facultatively anaerobic. Their colonies were yellow-orange or yellow due to the presence of carotenoid pigments. Summed feature 8 (C<sub>18:1</sub> $\omega$ 6c and/or C<sub>18:1</sub> $\omega$ 7c) and summed feature 3 (C<sub>16:1</sub> $\omega$ 6c and/or C<sub>16:1</sub> $\omega$ 7c) had been discovered as their major cellular fatty acids. Phosphatidylglycerol and phosphatidylethanolamine were the major known polar lipids.

The majority of bacteria in nature have not been cultivated in the laboratory yet [5]. They are likely to possess novel biosynthetic pathways and unknown biochemical characteristics and therefore could provide potential applications in biotechnology, agriculture,

and bioremediation [5]. Rock surfaces are challenging habitats for microbes due to the rapid changes in the intensity of radiation, temperature, water supply, and nutrient availability [6]. Aimed at investigating the unexplored bacterial lineages from the fully weathered granitic rock, a soil sample was collected from a rocky mountain in South China. In this study, we aimed to report the phenotypic, genetic, and chemotaxonomic features of the strain M6<sup>T</sup> to characterize it as a novel species in the genus *Sandaracinobacteroides*, with an emphasis on its ability to produce zeaxanthin, a coloring additive in the food industry and an essential micronutrient for humans. In addition, the sequences of the six aromatic ring-hydroxylating dioxygenases encoded by its genome were analyzed in detail in order to evaluate its potential ability to degrade organic pollutants.

## 2. Materials and Methods

### 2.1. Isolation and Maintenance of the Organisms

In 2019, the strain M6<sup>T</sup> was isolated from a soil sample collected on a rocky mountain in Changsha, Hunan province, South China (28.46° N, 113.18° E). For isolation, 5 g dried soil was taken in 250 mL Erlenmeyer flasks containing 45 mL of sterile 0.25% Ringer's solution (2.25 g NaCl, 0.105 g KCl, 0.045 g CaCl<sub>2</sub>, 0.05 g NaHCO<sub>3</sub> L<sup>-1</sup>) and agitated on a rotary shaker at 30 °C for 30 min. Subsequently, the suspension was serially diluted up to 10<sup>-5</sup> times. An aliquot of 0.2 mL of each of these dilutions was spread SSE/HD agar [7]. After six days of aerobic incubation at 30 °C, one yellow colony was transferred, purified, and designated as M6<sup>T</sup>. The isolates were sub-cultivated routinely on R2A (Reasoner's 2A) agar or modified RO (rich organic) medium (1 g yeast extract, 1 g Bacto peptone, 1 g sodium acetate, 0.3 g KCl, 0.5 g MgSO<sub>4</sub>·7H<sub>2</sub>O, 0.05 g CaCl<sub>2</sub>·2H<sub>2</sub>O, 0.3 g NH<sub>4</sub>Cl, 0.3 g K<sub>2</sub>HPO<sub>4</sub>, 20 µg vitamin B12, 15 g Bacto agar L<sup>-1</sup>) [8,9], and preserved in a glycerol solution (20%, v/v) at -80 °C. When compared with the sequences in the NCBI and EzBioCloud database, nearly half of the strains isolated from this soil sample showed the highest 16S rRNA gene sequence similarity below 98.7%, the threshold proposed for differentiating two species [10]. At that time, the M6<sup>T</sup> strain showed the highest similarity to the available sequence of *Sandaracinobacter sibiricus* (Table S1) and its sequenced genome was related to this genus (NCBI Reference Sequence: NZ\_CP059851.1). In this study, we compared the M6<sup>T</sup> strain with reference type strain *S. neustonicus* PAMCS 28131<sup>T</sup> and the recently described *Sandaracinobacteroides hominis* SZY PN-1<sup>T</sup>, purchased from the Japan collection of microorganisms and the Japanese national biologic resource center respectively, while *S. sibiricus* RB16-17 T was unavailable from any public culture collections [11].

### 2.2. Phenotypic and Biochemical Characteristics

Cell size and morphology of strain M6<sup>T</sup> grown in R2A for five days at 30 °C were studied by Hitachi SU8010 cold field scanning electron microscopy. The Gram reaction was determined by the standard Gram staining method. The motility of cells was performed by observing the growth spread of cells in test tubes containing semi-solid modified RO agar (0.3% w/v). Growth on modified RO and R2A agar at different temperatures (4, 10, 15, 20, 25, 30, 37, 42 °C) was observed. The pH range (pH 5.0–10.0 at intervals of 0.5 pH unit) for growth and tolerance to different NaCl concentration (0, 0.1, 0.2, 0.3, 0.4, 0.5, 1.0, 2.0, 3.0 and 5.0%, w/v) was assessed by using R2A and modified RO medium after incubation for one week. The pH of the media was adjusted with 10 mM MES (pH 5.0–6.0), 10 mM Tris (pH 7.0–9.0) or sodium carbonate/sodium bicarbonate (pH 10.0). Tests for hydrolysis of casein, starch, chitin, and Tweens (40, 60, 80) were performed using the methods described previously [12]. Catalase activity was examined by bubble production after application of 3% (v/v) H<sub>2</sub>O<sub>2</sub> solution to the isolated colony and oxidase activity was accessed by using 1% (v/v) *N, N, N', N'*-tetramethyl-1, 4-phenylenediamine reagent [13]. Other physiological, biochemical, and enzymatic activities were conducted by using API 20NE, API ID32, API ZYM, and API 50CH test kit (bioMérieux) according to the manufacturer's instructions. Cells grown on the modified RO agar plates at 30 °C for three days were employed for API tests.

For determining the presence of bacteriochlorophyll *a* and carotenoid pigment, cells were harvested and extracted with an acetone-methanol mixture. The supernatant was detected for absorbance at different wavelengths on a spectrophotometer (Pgeneral, T6) [11]. High-resolution mass spectrometry (HRMS) was carried out on an Agilent 6545 Quadrupole Time of Flight (Q-TOF) high-resolution mass spectrometer equipped with a reverse phase C18 column (Agilent, Eclipse Plus, 1.8  $\mu\text{m}$  50  $\times$  2.1 mm), running in positive ionization mode with a resolution of 30,000. The flow rate was set at 0.3 mL/min with a mobile phase of H<sub>2</sub>O/ACN each containing 0.1% of formic acid. The ACN percentage gradually increased from 5% to 95% in 12 min. The injection volume was 2  $\mu\text{L}$ . Voges-Proskauer (VP) reaction was tested as previously described [12] with *Escherichia coli* and *Enterobacter aerogenes* as negative and positive control respectively. H<sub>2</sub>S production assay was performed using triple sugar iron agar.

### 2.3. Chemotaxonomic Analysis

The polar lipids were analyzed using freeze-dried cells as described by Minnikin et al., 1984 [14]. Fatty acid methyl esters were prepared according to the standard MIDI protocol (Sherlock Microbial Identification System, version 6.0B) and identified by using the MIDI with the TSBA database version 6.1. Isoprenoid quinones were analyzed by using reversed-phase HPLC as described by Shin, et al. 1996 [15].

### 2.4. The 16S rRNA Gene Sequencing and Phylogenetic Analysis

The 16S rRNA gene of strain M6<sup>T</sup> was amplified by PCR using forward primer 27F and reverse primer 1492R [16] and sequenced with an Applied Biosystem 3730XL DNA analyzer. The closest phylogenetic neighbors of this sequence were identified by using BLASTN search program at the NCBI website (<https://blast.ncbi.nlm.nih.gov/Blast.cgi> (accessed on 19 July 2022)) and the EZBioCloud server [17]. The 16S rRNA gene sequence of the strain M6<sup>T</sup> was subjected to multiple alignments with the sequences of the closely related bacteria by using CLUSTAL  $\Omega$  [18]. Gaps at the 5' and 3' ends were deleted using the software package BioEdit. Phylogenetic trees were reconstructed by using three different methods, the neighbor-joining method [19], the maximum-likelihood algorithm [20], and the minimum-evolution method [21] with the MEGA7 program [22]. During the phylogenetic analysis, evolutionary distances were calculated using Kimura's two-parameter model [23], and bootstrap values were calculated based on 1000 replications [24].

### 2.5. Complete Genome Sequencing and Phylogenomic Analysis

Genomic DNA was extracted by a standard phenol-chloroform method and further purified by AMPure XP beads (Beckman Coulter, Brea, CA, USA) and then quantified and quality controlled using a Qubit 2.0 fluorometer (Thermo Fisher Scientific, Waltham, MA, USA), NanoDrop software and agarose gel electrophoreses [25]. High-molecular-weight DNA was isolated using a BluePinppin system (Sage Science, Beverly, MA, USA). Approximately 1.5  $\mu\text{g}$  of genomic DNA was used for library construction using a one-dimensional (1D) ligation sequencing kit (SQK-LSK109 kit; Oxford Nanopore, Oxford, UK). No size selection or shearing was applied. The library was loaded into an R9.4 flow cell for the PromethION platform (PromethION flow cells, FLO-PRO002; Oxford Nanopore). Nanopore quality control was achieved with a threshold value (Q) of 7. Illumina sequencing was performed on the NovaSeq PE150 instrument at the Wuhan Benagen Co. Ltd. (Wuhan, China) Low-quality bases (quality value,  $\leq 30$ , account for only 9.0%), and were removed. De novo assembly in combination with the Illumina short reads and ONT long reads was conducted using SPAdes 3.10.0, Unicycler 0.4.8., Racon, Miniasm and Pilon1.22.

Digital DNA-DNA hybridization (dDDH) values were determined by using the genome-to-genome distance calculator (GGDC 2.1) at <http://ggdc.dsmz.de> (accessed on 2 July 2022) [26]. The average nucleotide identity (ANI) was calculated using OrthoANI with default parameters on the website [27]. For phylogenetic analysis of core proteome, the extraction of the core proteome from the genomic sequence was automati-

cally executed based on the M1CR0B1AL1Z3R pipeline (<https://github.com/orenavr/microbializer> (accessed on 2 July 2022)) with the default parameters as described by [28]. A phylogenomic tree based on a bacterial core gene set was reconstructed with the genome sequences of the isolate and its closely related species, using an automated multi-locus species tree (autoMLST) pipeline (<https://automl.st.ziemertlab.com/> (accessed on 7 July 2022)) [29]. Conserved proteins shared between strain pairs were estimated based on the percentage of conserved proteins (POCP), which were calculated as the algorithm  $[(C1 + C2)/(T1 + T2)] \times 100\%$  [30]. The average amino acid identity (AAI) was obtained from the website <http://enve-omics.ce.gatech.edu/aai/> (accessed on 5 September 2022) [31].

### 3. Results and Discussion

#### 3.1. Phylogenetic Placement and Phylogenomics

An almost complete 16S rRNA gene sequence of strain M6<sup>T</sup> (1407 nucleotides) was deposited in GeneBank under accession number ON876070. Sequence analysis by BLASTN and on the EzBioCloud database revealed the highest similarity of 96.3% to *S. hominis* SZY PN-1<sup>T</sup>, followed by *S. sibiricus* RB16-17<sup>T</sup> and *S. neustonicus* PAMC 28131<sup>T</sup> with a similarity of 95.5% and 95.1%, respectively, all below the proposed threshold 98.7% for differentiating two species [10] but above the minimum identity value that guarantees the circumscription of a single genus [32]. Other closely related genera were *Sphingomonas* ( $\leq 94.6\%$ ), *Sandaracinorhabdus* ( $\leq 93.8$ ), and *Polymorphobacter* ( $\leq 93.8\%$ ). The phylogenetic analyses based on 16S rRNA gene sequences demonstrated that strain M6<sup>T</sup> formed a distinct lineage in a stable clade with the two *Sandaracinobacter* species and the *S. hominis* in the maximum-likelihood phylogenetic tree (Figure 1), and this relationship was also supported by the neighbor-joining and minimum-evolution trees (Figures S1 and S2).

To further prove that strain M6<sup>T</sup> should be placed in the genus *Sandaracinobacteroides* other than establishing a new genus, we calculated the POCP (percentage of conserved proteins) and AAI values between M6<sup>T</sup> and its phylogenetic relatives. As summarized in Table 1, they were all above the established cut-off values for genus delineation of 50% and 60% respectively [30,31].

In order to establish a more specific taxonomic position at the species level, genome comparison was performed between M6<sup>T</sup> and its phylogenetic relatives first using ANI (Average Nucleotide Identity) and dDDH (digital DNA-DNA Hybridization) value calculation (Table 1). The levels of dDDH between M6<sup>T</sup> and its phylogenetic relatives were far below the threshold value of 70% for assigning strains to the same genomic species. The ANI values were also under the proposed cut-off ANI values of 95–96% for demarcating bacterial species [33]. Moreover, maximum-likelihood phylogenetic trees based on either the core proteome or the 80 core genes from the autoMLST analysis both revealed a separate lineage for strain M6<sup>T</sup> (Figures 2 and S3). These consistent results indicated that strain M6<sup>T</sup> represented a new member of the genus *Sandaracinobacteroides*.

**Table 1.** The 16S rRNA gene similarity, POCP, AAI, ANI, and dDDH values between M6<sup>T</sup> and its closely related strains available with genome sequence.

Strains Pair	16S% Identity	POCP Value	AAI	dDDH	ANI
M6 <sup>T</sup> vs. <i>Sandaracinobacteroides hominis</i>	96.3%	80.7%	62.1%	18.0%	72.6%
M6 <sup>T</sup> vs. <i>Sandaracinobacter neustonicus</i>	95.1%	79.2%	62.4%	18.4%	72.9%
<i>S. hominis</i> vs. <i>S. neustonicus</i>	96.6%	88.2%	74.2%	21.1%	77.2%

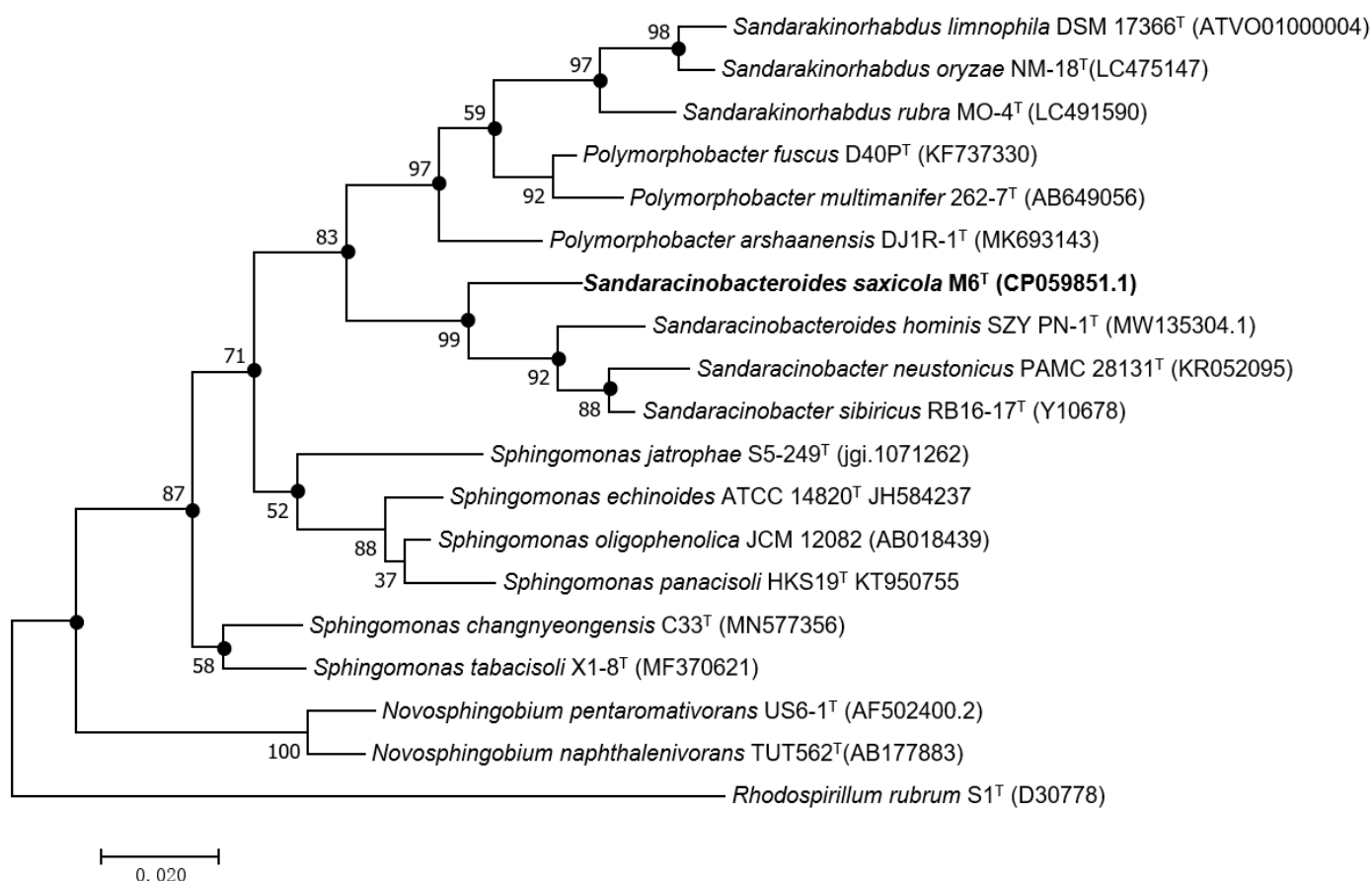


**Figure 1.** Maximum-likelihood phylogenetic tree based on 16S rRNA gene sequence of strain M6<sup>T</sup> and other related species. Bootstrap values (expressed as a percentage of 1000 replications) above 50% are shown at the branch points. Filled circles at nodes, denotes branches recovered using the neighbor-joining and minimum-evolution methods. *Rhodospirillum rubrum* S1<sup>T</sup> was used as an out group. Bar 0.02 substitutions per nucleotide position (*S. saxicola*, see Section 3.6).

In spite that *Sandaracinobacteroides hominis* SZY PN-1<sup>T</sup> and *Sandaracinobacter neustonicus* PAMC 28131<sup>T</sup> were placed in two genera, the values based on genome and proteome comparison between these two strains (Table 1) were actually above the threshold limits for delineation of the bacterial genus.

Venn diagram generated from the genome comparative studies of *S. saxicola* M6<sup>T</sup>, *S. hominis* SZY PN-1<sup>T</sup>, and *S. neustonicus* PAMC 28131<sup>T</sup> using the OrthoVenn2 tool further demonstrated that the three species form a total of 2718 clusters, of which 1071 orthologous clusters (at least contains two species) and 1647 are single-copy gene clusters. The *S. saxicola* M6<sup>T</sup> contains 50 unique clusters, some of which are involved in cellular aromatic compound or heterocycle metabolic process (Figure 3). Overall genome sequence identity between these three strains is shown in Figure 4.

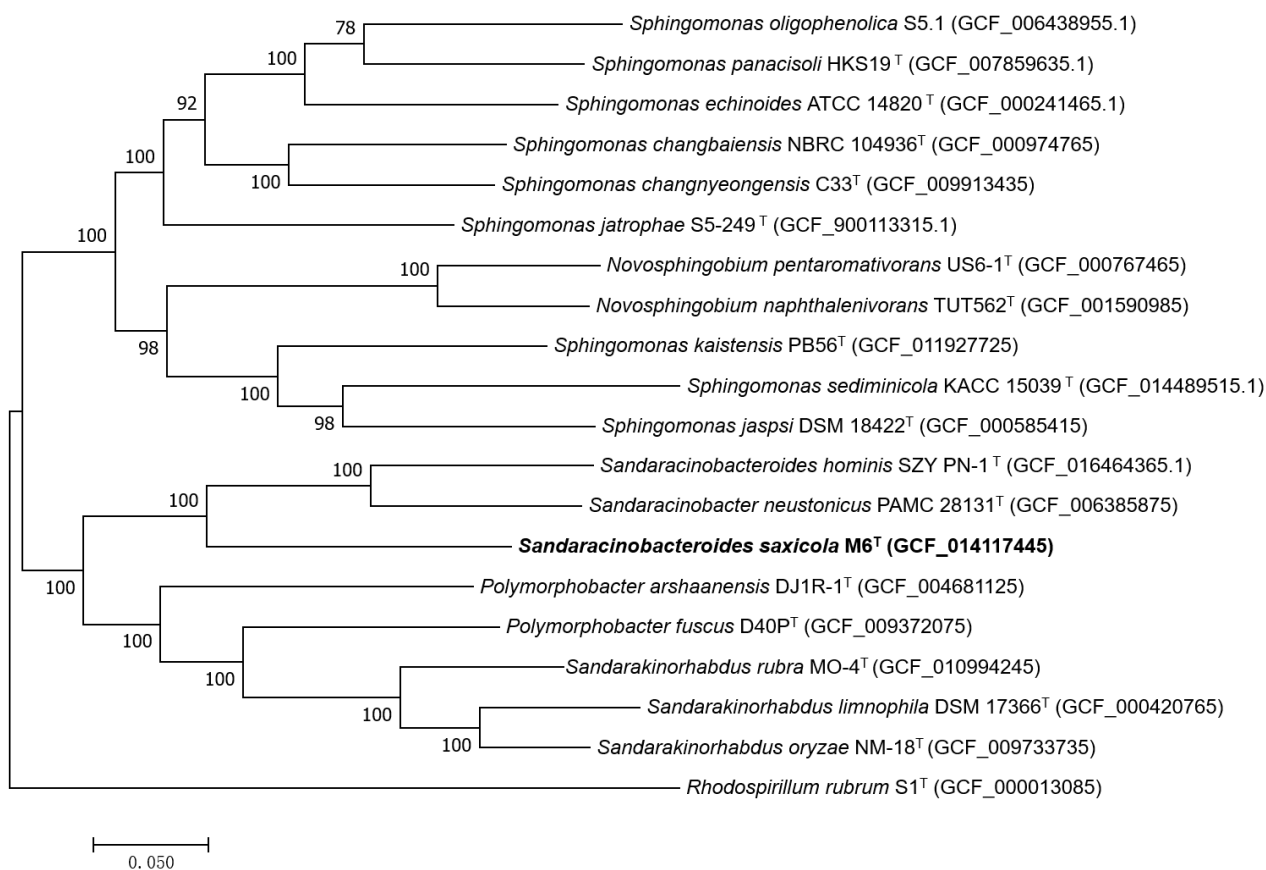


**Figure 2.** Maximum-likelihood phylogenetic tree based on the core genome indicating the phylogenetic positions of strains M6<sup>T</sup> with the related species. The scale bar indicates 0.020 substitutions per nucleotide position. *Rhodospirillum rubrum* S1<sup>T</sup> (GCF\_000013085) was used as an out group. GenBank accession numbers are listed for each sequence in parentheses.

### 3.2. Morphology and Metabolic Profile

Cells of M6<sup>T</sup> were Gram-negative, aerobic, long rod-shaped, with a size of 0.5–0.6 × 1.1–1.3 μm (Figure 5). Colonies grew in a circular, convex, opaque manner with detectable yellow pigmentation on the modified RO and R2A agar plates. Growth was observed at temperatures of 15–37 °C and pH 6.0–9.0, with optimal growth at 30 °C and pH 6.0–8.5. Strain M6<sup>T</sup> was sensitive to NaCl, growth was inhibited by NaCl (≥0.1% (w/v)). Unlike the *Sphingomonas oligophenolica* JCM 12082<sup>T</sup>, a halo-sensitive soil bacterium with a 16S rDNA sequence similarity of 94.6% to M6<sup>T</sup>, this inhibition could not be recovered by 6 mM CaCl<sub>2</sub> [35].

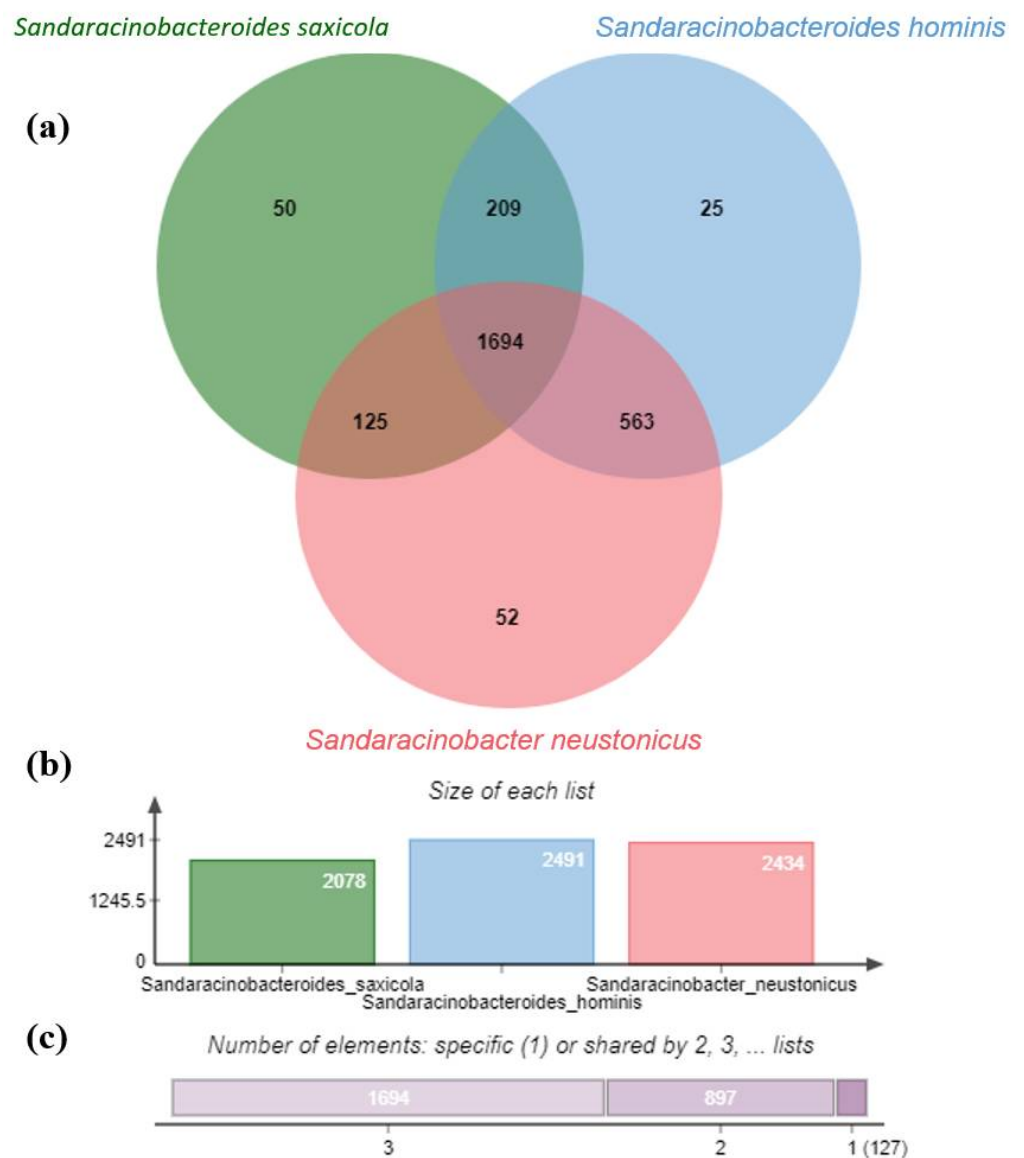


**Figure 3.** Venn diagram and the bar plots generated by Orthovenn2 represent the distribution of shared and unique gene clusters amongst *S. saxicola* M6<sup>T</sup>, *S. hominis* SZY PN-1<sup>T</sup>, and *S. neustonicus* PAMC 28131<sup>T</sup>. **(a)** The Venn diagram represents the distribution of core ortholog clusters, shared clusters, and unique clusters in all three species. **(b)** The bar plot represents the cumulative ortholog clusters found in each species. **(c)** The bar plot illustrates the cumulative core, shared, and unique clusters in all the three species, where label 1 on the horizontal scale shows the cumulative number of unique clusters (127) for all the three species, while label 2 shows the total number of clusters shared by two species (897) and so on.

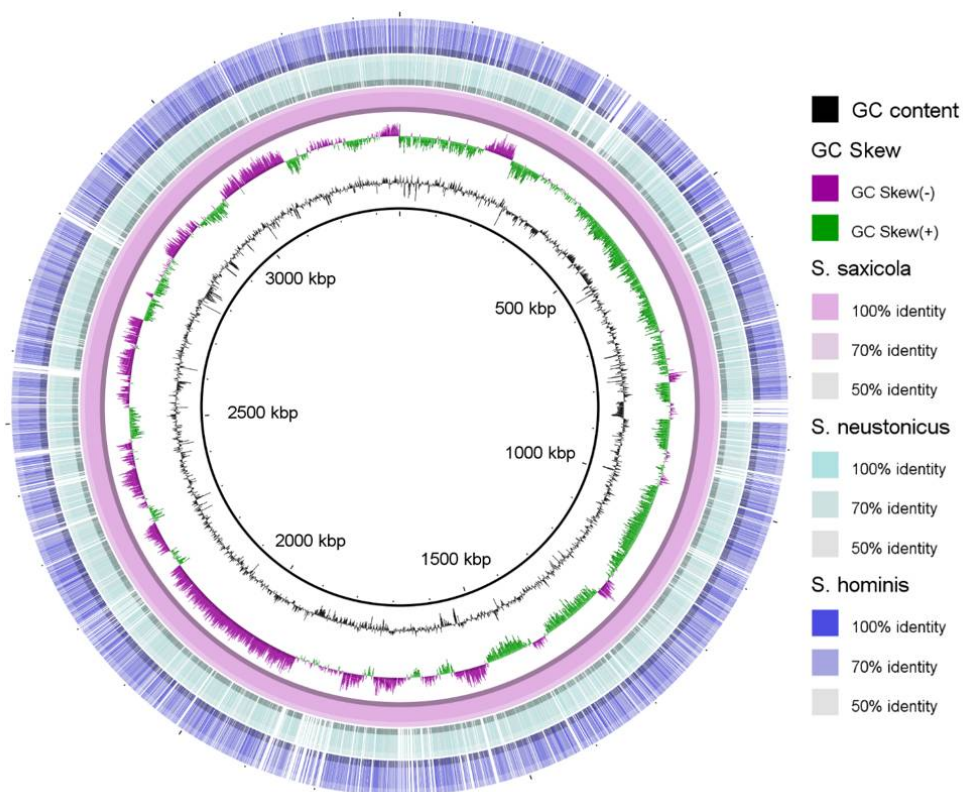


**Figure 4.** Overall genome sequence identity distribution between *S. saxicola* M6<sup>T</sup>, *S. hominis* SZY PN-1<sup>T</sup>, and *S. neustonicus* PAMC 28131<sup>T</sup>. Location in the reference genome is indicated by numeration on the inside of the ring. GC content in the reference genome is indicated by the black bar graphs between the genomic coordinates and the colored ring. The graphical view of the alignments was rendered using the BLAST Ring Image Generator (BRIG) [34].

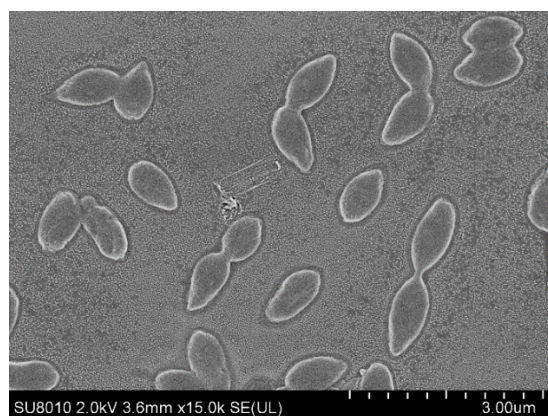


**Figure 5.** Scanning electron microscopy image showing the cell morphology of strain M6<sup>T</sup>.

Though the two *Sandaracinobacter* species *S. sibiricus* RB16-17<sup>T</sup> and *S. neustonicus* PAMC 28131<sup>T</sup> were listed as invalid names, we still included them together with *Sandaracinobacteroides hominis* SZY PN-1<sup>T</sup> as reference strains for a comprehensive phenotypic, genomic and chemotaxonomic properties comparison. Moreover, our data based on phylogenomics analysis also implied that *Sandaracinobacter neustonicus* PAMC 28131<sup>T</sup> and *Sandaracinobacteroides hominis* SZY PN-1<sup>T</sup> should be placed in a single genus. In contrast to *S. sibiricus* RB16-17<sup>T</sup>, strain M6<sup>T</sup>, *S. hominis* SZY PN-1<sup>T</sup>, and *S. neustonicus* PAMC 28131<sup>T</sup> all did not contain the bacteriochlorophyll a, a main feature of the genus *Sandaracinobacter* [11]. A major carotenoid peak of 424 nm was also not detected in these three strains (Figure S4).

According to the API tests and other biochemical assays, both strains M6<sup>T</sup> and *S. hominis* SZY PN-1<sup>T</sup> were positive for catalase and trypsin, and hydrolyzed starch and aesculin. Unlike *S. hominis* SZY PN-1<sup>T</sup>, strain M6<sup>T</sup> was negative for  $\alpha$ -chymotrypsin, esterase (C4), and esterase lipase (C8), and consequently does not hydrolyze Tweens (40, 60, and 80), however, it was positive for valine arylamidase, cystine arylamidase,  $\alpha$ -galactosidase,  $\beta$ -Galactosidase (Table 2). In short, the strain M6<sup>T</sup> maintained commonality within this genus in many respects, while also preserving many unique characteristics that could differentiate it from the related strains.

**Table 2.** Phenotypic characteristics distinguishing strains M6<sup>T</sup> from other species of the genus *Sandaracinobacteroides* and *Sandaracinobacter*.

Characteristics	1	2	3	4
Oxygen requirement	Aerobic	Obligately aerobic	Facultatively anaerobic	Strictly aerobic
Growth at/with: NaCl (% w/v)	0	0–1.0	0.5–1.0	0–1.0
Temperature (optimum) (°C)	15–37 (30)	10–37 (30)	4–37 (30)	(25–30)
pH range (optimum)	6.0–9.0 (6.0–8.5)	6.0–8.0 (7.0)	6.0–8.0 (6.5–7.0)	(7.5–8.5)
Motility	+	–	–	+
Bacteriochlorophyll a	–	–	–	+
Major carotenoid peaks (nm)	450, 474	452, 478	450, 474	424, 450, 474
Catalase activity	+	+	+	–
Oxidase activity	–	–	+	+
Hydrolysis of: Starch	+	+	+	–
Tweens (80)	–	–	+	ND
Quinone(s)	Q-9, Q-10	Q-10, Q-11	Q-10	Q-9, Q-10
DNA G+C content (mol %)	67.7%	65.0%	65.3%	68.5% *
Enzyme activities: Esterase lipase (C8)	–	weakly	–	ND
Esterase (C4)	–	+	–	ND
Valine arylamidase	+	–	ND	ND
Cystine arylamidase	+	–	ND	ND
$\alpha$ -chymotrypsin	–	weakly	+	ND
$\alpha$ -Galactosidase	+	–	–	ND
$\beta$ -Galactosidase	+	–	+	ND
Acid production from: Aesculin	+	+	–	ND
D-Maltose	–	–	+	ND
Potassium 5-ketogluconate	–	–	+	ND
Main polar lipids	PG, PE, PL1–4, GL, L1-4	DPG, PE, PG, SGL1-2, GL1-4, L1-7	PG, PE, PL1–2, AL, GL, L	ND

Strains: 1, M6<sup>T</sup> (this study); 2, *Sandaracinobacteroides hominis* SZY PN-1<sup>T</sup> (data from Qu et al. [1]); 3, *S. neustonicus* PAMC 28131<sup>T</sup> (this study); 4, *S. sibiricus* RB16-17<sup>T</sup> (data from Yurkov et al. [2,11]). +, Positive; –, Negative. ND, could not be detected because the strain was unavailable from any public culture collection center. \* Thermal denaturation method [2].

### 3.3. Chemotaxonomic Characteristics

Cellular fatty acids profiles of M6<sup>T</sup>, *Sandaracinobacteroides hominis* SZY PN-1<sup>T</sup>, and *S. neustonicus* PAMC 28131<sup>T</sup> are depicted in Table S2. The predominant fatty acids (relative account > 10%) of the novel isolate were C<sub>18:1</sub> $\omega$ 7c, summed feature 3, C<sub>14:0</sub> 2-OH, and C<sub>16:0</sub>, whereas both *Sandaracinobacteroides hominis* SZY PN-1<sup>T</sup> and *S. neustonicus* PAMC 28131<sup>T</sup> contained summed feature 3, 8 and C<sub>17:1</sub> $\omega$ 6c as the major fatty acids.

In consistent with *S. hominis* SZY PN-1<sup>T</sup> and *S. neustonicus* PAMC 28131<sup>T</sup>, phosphatidylglycerol (PG) and phosphatidylethanolamine (PE) have been determined as the

predominant polar lipids of strain M6<sup>T</sup>. In comparing with *S. hominis* SZY PN-1<sup>T</sup>, which additionally included one diphosphatidylglycerol (DPG), two sphingoglycolipids (SGL), four unidentified glycolipids (GL), and seven unidentified lipids (L) as the major polar lipids, strain M6<sup>T</sup> contained four unidentified phospholipids (PL), four unidentified lipids (L) and an unidentified glycolipid (GL) (Figure S5).

### 3.4. The Biosynthesis of Zeaxanthin

The assembled genome sequence of strain M6<sup>T</sup> had a length of 3,364,212 bp and a GC content of 67.7% (Figure S6). Genome annotation by the NCBI Prokaryotic Genome Annotation Pipeline 4.12 (PGAP) predicted a total of 3375 genes with 3298 coding sequences and 49 RNA genes (three rRNAs, 43 tRNAs, and three noncoding RNAs).

AntiSMASH [36] analysis of the genome detected a gene cluster for zeaxanthin biosynthesis. This gene cluster contains three genes located adjacent to each other. They encoded the phytoene synthase (RS11760), phytoene desaturase (RS11765), lycopene beta-cyclase (RS11770) respectively. The gene for beta-carotene hydroxylase (RS12330), the enzyme responsible for the last step in zeaxanthin biosynthesis was found upstream of the gene cluster (Figure 6a,b). The presence of zeaxanthin was subsequently confirmed by HRMS (high-resolution mass spectrum), in which a protonated molecular ion at  $m/z$  568.4260 [M+H]<sup>+</sup> (calcd. for C<sub>40</sub>H<sub>56</sub>O<sub>2</sub>, 568.4280, 3.5 ppm) was observed (Figure 6c).

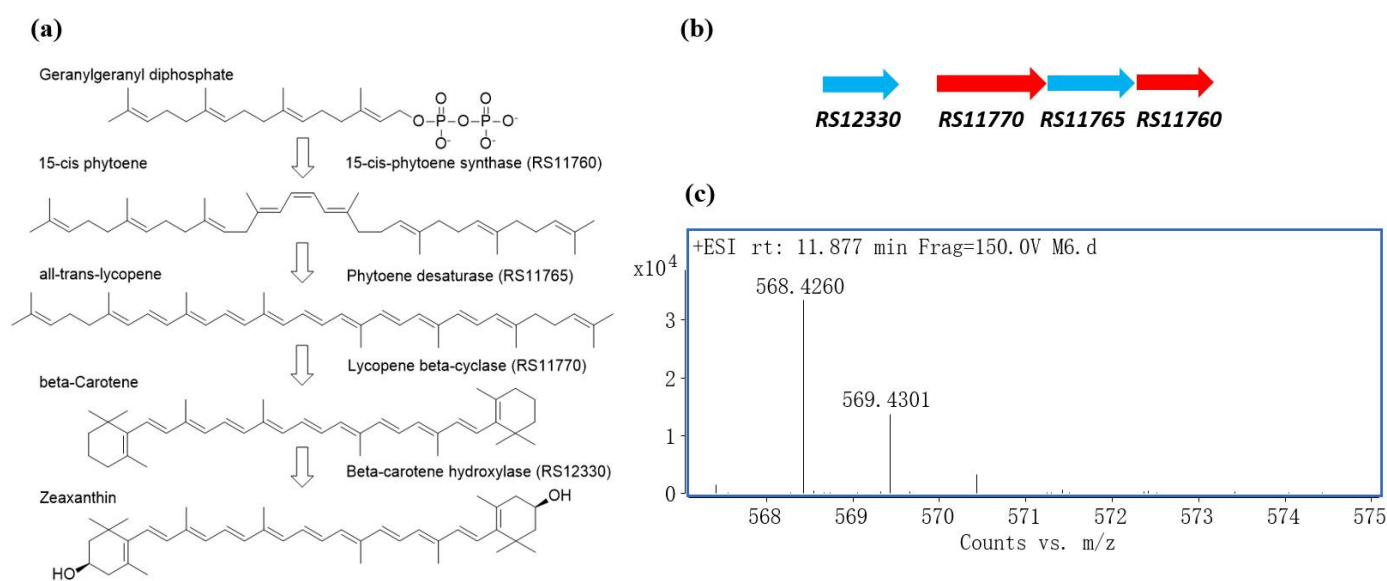


**Figure 6.** Zeaxanthin production by M6<sup>T</sup>. (a) Zeaxanthin biosynthesis pathway. (b) Zeaxanthin biosynthesis gene cluster found in the genome of M6<sup>T</sup>. (c) HRMS chromatogram of zeaxanthin in the acetone-methanol extract of M6<sup>T</sup>.

### 3.5. Multiple Copies of Aromatic Ring-Hydroxylating Dioxygenases

According to the PGAP annotation, the genome of M6 also contained six genes encoding aromatic ring-hydroxylating dioxygenases (ARHD), the enzyme involved in the first and rate-limiting step of aerobic biodegradation of aromatic compounds [37]. Multiple sequence alignment demonstrated they all had a conserved Rieske [2Fe–2S] center and a C-terminal catalytic domain (Figure 7). Further analysis of Pfam indicated that these enzymes are homotrimers and are distantly related to the typical oxygenase [38].

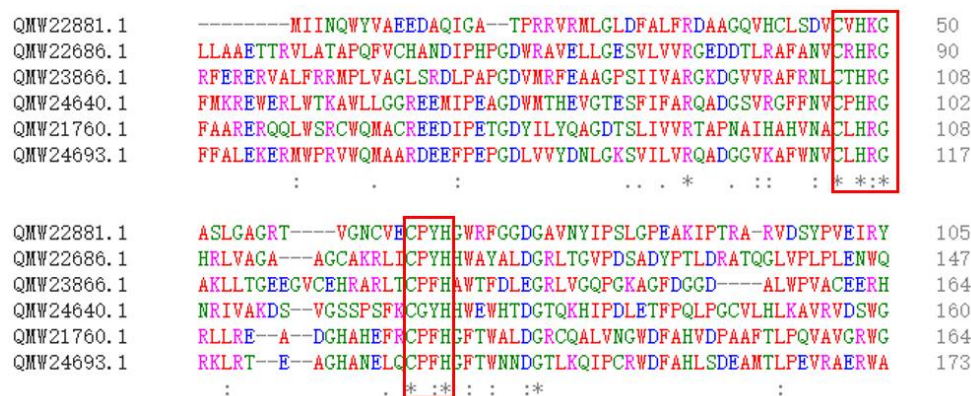


**Figure 7.** Amino acid sequence alignment of the six ARHDs showing the consensus pattern: C-x-H-R-[GAR]-x(7,8)-[GEKVI]-[NERAQ]-x(4,5)-C-x-[FY]-H, in which the 2 C's and the 2 H's are 2Fe-2S ligands [39]. Asterisks (\*) indicate positions which have a single, fully conserved residue, a: (colon) indicates conservation between groups of strongly similar properties, a. (period) indicates conservation between groups of weakly similar properties.

Subsequently, ClassicRAST-based functional gene subsystem clustering analysis revealed 19 ORFs involved in the metabolism of aromatic compounds (Figure S7) [40]. Considering that the *Sphingomonas oligophenolica* JCM 12082<sup>T</sup>, a strain with a 16S rDNA sequence similarity of 94.6% to M6<sup>T</sup>, was reported to degrade phenolic acids at low concentrations [35], and it has only 10 ORFs classified into the class for the metabolism of aromatic compounds, we speculate that the strain M6<sup>T</sup> might be able to degrade some unusual aromatic compounds.

### 3.6. Description of *Sandaracinobacteroides saxicola* sp. nov.

sa.xi'co.la, L. neut. n. saxum rock, L. masc./fem. Suffix n. -cola inhabitant, N.L. masc./fem. n. (nominative in apposition) saxicola rock dweller.

Cells are Gram-negative, motile, and long rod-shaped with a width of 0.5–0.6 µm and a length of 1.1–1.3 µm. The colonies are round convex, opaque, and in yellow color. Growth is observed on R2A agar at 15–37 °C (optimum, 30 °C), and at pH 6.0–9.0 (optimum 6.0–8.5). Growth occurs in the absence of NaCl. Negative for VP reaction, H<sub>2</sub>S production, and oxidase activities. Positive for catalase activities. Xanthine, hypoxanthine and Tweens (40, 60 and 80) are not hydrolyzed, but casein and starch are hydrolyzed. According to the API ZYM test, strain M6<sup>T</sup> is positive for alkaline phosphatase, trypsin, acid phosphatase, naphthol-AS-BI-phosphohydrolase, α-galactosidase and α-glucosidase, β-glucosidase, leucine arylamidase, β-galactosidase, N-acetyl-β-glucosaminidase, valine arylamidase, cystine arylamidase, α-fucosidase, but negative for esterase (C4), esterase lipase (C8), lipase (C14), α-chymotrypsin, β-glucuronidase. In API 20NE test strips, this novel isolated was positive for aesculin hydrolysis and β-galactosidase, but negative for nitrate reduction to nitrite, nitrite reduction, urease, indole production, acidification of glucose, arginine dihydrolase, and gelatin hydrolysis. In the API 50CH test, acid was produced from aesculin, 5-ketogluconate, sucrose and maltose, DL-arabinose, starch, melezitose, but not from 2-ketogluconate, N-acetylglucosamine, D-adonitol, amygdalin, DL-arabitol, arbutin, cellobiose, dulcitol, erythritol, D-fructose, DL-fucose, D-galactose, gentiobiose, D-glucose, glycerol, glycogen, inositol, inulin, lactose, D-lyxose, D-mannitol, D-mannose, melibiose, methyl α-D-glucopyranoside, methyl α-D-mannopyranoside, methyl β-D-xylopyranoside, potassiumgluconate, raffinose, L-rhamnose, D-ribose, salicin, D-sorbitol, L-sorbose, D-tagatose, trehalose, turanose, xylitol or DL-xylose. Cell could assimilate sucrose, maltose, L-alanine, L-serine, glycogen, D-glucose, 3-hydroxybutyrate, L-proline, but not assimilate adipate, 3-hydroxybenzoate, acetate, N-acetylglucosamine, L-arabinose, citrate, L-fucose, caprate, L-histidine, inositol, itaconate, 2-ketogluconate, 5-ketogluconate, lactate, malonate, D-mannitol, D-melibiose, phenylacetate, propionate, L-rhamnose, D-ribose, salicin,

D-sorbitol, suberate, gluconate, D-mannose, 4-hydroxybenzoate, malate or valerate (according to API 20NE and API ID 32GN test strips).

*Sandaracinobacteroides saxicola* sp. nov. was deposited in the China General Microbiological Culture Collection Center (CGMCC 1.19164) and the NITE Biological Resource Center (NBRC 115420) in Japan.

#### 4. Conclusions

The 16S rRNA gene sequence similarity, POCP, and AAI values between strain M6<sup>T</sup> and type strains in genus *Sandaracinobacteroides*, were all below the prescribed threshold for differentiating two species but above the established cut-off values for genus delineation [26,33]. Phylogenetic analysis based on 16S rRNA gene sequence and core proteome showed that strain M6<sup>T</sup> was close to species in genera *Sandaracinobacteroides* and *Sandaracinobacter* but had obvious genetic distance. Furthermore, the discrepancies in the physiological, biochemical, and chemotaxonomic characteristics also could clearly differentiate M6<sup>T</sup>, and from the closely related species. In conclusion, we suggest that strain M6<sup>T</sup> represents a novel species of the genus *Sandaracinobacteroides*, for which the name *Sandaracinobacteroides saxicola* sp. nov. is proposed.

In addition, we testified that zeaxanthin was one of the carotenoid pigments produced by M6<sup>T</sup>. In view of its application in the food and pharmaceutical industry, strain M6<sup>T</sup> could be an attractive candidate for the production of zeaxanthin. Moreover, according to the ARHD sequence analysis, strain M6<sup>T</sup> could also be used in controlling organic pollution when applied alone or in combination with other strains.

**Supplementary Materials:** The following supporting information can be downloaded at: <https://www.mdpi.com/article/10.3390/d14100807/s1>, Table S1: The 16S rRNA gene sequence analysis of the isolated strains. Table S2: Cellular fatty acid composition (%) of M6<sup>T</sup>, *S. hominis* SZY PN-1<sup>T</sup>, and *S. neustonicus* PAMC 28131<sup>T</sup>. Figure S1: Neighbor-Joining tree based on the 16S rRNA gene sequences of strain M6<sup>T</sup> and representatives of related taxa. Figure S2: Minimum-evolution tree based on the 16S rRNA gene sequences of strain M6<sup>T</sup> and representatives of related taxa. Figure S3: Maximum-likelihood phylogenetic tree based on the core proteome indicating the phylogenetic positions of strains M6<sup>T</sup> with the related species. Figure S4: Total pigment absorption spectra of strain M6<sup>T</sup>. Figure S5: Two-dimensional TLC plate image of total polar lipids of strain M6<sup>T</sup> sprayed with phosphomolybdic acid. Figure S6: Circular map of the chromosome of strain M6<sup>T</sup>. Figure S7: Subsystem category distribution from strain M6<sup>T</sup>, generated through ClassicRAST pipeline (default settings).

**Author Contributions:** Conceptualization, Y.T. and Q.L. (Qingshu Liu); formal analysis, Y.T., Q.L. (Qingshan Long) and C.Z.; investigation, Y.T. and C.Z.; writing—original draft preparation, Y.T. and C.Z.; writing—review and editing, Q.L. (Qingshu Liu), Z.G. and Y.T.; supervision, P.L., Z.G. and Q.L. (Qingshu Liu); funding acquisition, Y.T., Z.G. and Q.L. (Qingshan Long). All authors have read and agreed to the published version of the manuscript.

**Funding:** This study was supported by State Key Laboratory of Microbial Technology Open Projects Fund (M2021-10), Hunan Provincial Natural Science Foundation (2021JJ40306), National Natural Science Foundation (32000047), The Science and Technology Project of Hunan Province (2021NK1040), and Hunan Provincial Science & Technology Department Project (2020NK2006).

**Institutional Review Board Statement:** Not applicable.

**Data Availability Statement:** The DDBJ/EMBL/GenBank accession number for the 16S rRNA gene sequence and the complete genome sequence of *Sandaracinobacteroides* sp. M6 are ON876070 and CP059851.1 respectively. The SRA (Sequence Read Archive) raw data is available under accession number SRR12366083. The Biosample and BioProject accession numbers are SAMN15676387 and PRJNA649658 respectively.

**Conflicts of Interest:** The authors declare no conflict of interest.

## References

1. Qu, P.H.; Luo, H.M. *Sandaracinobacteroides hominis* gen. nov., sp. nov., isolated from human skin. *Arch. Microbiol.* **2021**, *203*, 5067–5074. [[CrossRef](#)] [[PubMed](#)]
2. Yurkov, V.; Stackebrandt, E. Reorganization of the genus *Erythromicrobium*: Description of “*Erythromicrobium sibiricum*” as *Sandaracinobacter sibiricus* gen. nov., sp. nov., and of “*Erythromicrobium ursincola*” as *Erythromonas ursincola* gen. nov., sp. nov. *Int. J. Syst. Bacteriol.* **1997**, *47*, 1172–1178. [[CrossRef](#)]
3. Lee, I.; Jang, I.G. *Sandaracinobacter neustonicus* sp. nov., isolated from the sea surface microlayer in the southwestern pacific ocean, and emended description of the genus *Sandaracinobacter*. *Int. J. Syst. Evol. Microbiol.* **2020**, *70*, 4698–4703. [[CrossRef](#)] [[PubMed](#)]
4. Parte, A.C.; Sardà Carbasse, J. List of prokaryotic names with standing in nomenclature (LPSN) moves to the dsmz. *Int. J. Syst. Evol. Microbiol.* **2020**, *70*, 5607–5612. [[CrossRef](#)] [[PubMed](#)]
5. Overmann, J.; Abt, B. Presence and future of culturing bacteria. *Annu. Rev. Microbiol.* **2017**, *71*, 711–730. [[CrossRef](#)]
6. Gueidan, C.; Villaseñor, C.R. A rock-inhabiting ancestor for mutualistic and pathogen-rich fungal lineages. *Stud. Mycol.* **2008**, *61*, 111–119. [[CrossRef](#)]
7. Pascual, J.; Wüst, P.K. Novel isolates double the number of chemotrophic species and allow the first description of higher taxa in *Acidobacteria* subdivision 4. *Syst. Appl. Microbiol.* **2015**, *38*, 534–544. [[CrossRef](#)]
8. Maltman, C.; Yurkov, V. The effect of tellurite on highly resistant freshwater aerobic anoxygenic phototrophs and their strategies for reduction. *Microorganisms* **2015**, *3*, 826–838. [[CrossRef](#)]
9. Yurkov, V.V.; Krieger, S. *Citromicrobium bathyomarimum*, a novel aerobic bacterium isolated from deep-sea hydrothermal vent plume waters that contains photosynthetic pigment-protein complexes. *J. Bacteriol.* **1999**, *181*, 4517–4525. [[CrossRef](#)]
10. Kim, M.; Oh, H.S. Towards a taxonomic coherence between average nucleotide identity and 16s rna gene sequence similarity for species demarcation of prokaryotes. *Int. J. Syst. Evol. Microbiol.* **2014**, *64*, 346–351. [[CrossRef](#)]
11. Yurkov, V.; Gorlenko, V. *Erythrobacter sibiricus* sp. nov., a new fresh-water aerobic bacterial species containing bacteriochlorophyll a. *Microbiology* **1990**, *59*, 85–89.
12. Smibert, R.M.; Krieg, N.R. Phenotypic characterization. In *Methods for General Molecular Bacteriology*; Gerhardt, P., Murray, R.G.E., Eds.; American Society for Microbiology: Washington, DC, USA, 1994; pp. 607–654.
13. Kovacs, N. Identification of *Pseudomonas pyocyanea* by the oxidase reaction. *Nature* **1956**, *178*, 703. [[CrossRef](#)] [[PubMed](#)]
14. Minnikin, D.E.; O'Donnell, A.G. An integrated procedure for the extraction of bacterial isoprenoid quinones and polar lipids. *J. Microbiol. Methods* **1984**, *2*, 233–241. [[CrossRef](#)]
15. Shin, Y.K.; Lee, J.S. Isoprenoid quinone profiles of the *Leclercia adecarboxylata* KCTC 1036<sup>T</sup>. *J. Microbiol. Biotechnol.* **1996**, *6*, 68–69.
16. Frank, J.A.; Reich, C.I. Critical evaluation of two primers commonly used for amplification of bacterial 16s rRNA genes. *Appl. Env. Microbiol.* **2008**, *74*, 2461–2470. [[CrossRef](#)]
17. Yoon, S.H.; Ha, S.M. Introducing ezbiocloud: A taxonomically united database of 16s rna gene sequences and whole-genome assemblies. *Int. J. Syst. Evol. Microbiol.* **2017**, *67*, 1613–1617. [[CrossRef](#)]
18. Sievers, F.; Higgins, D.G. Clustal omega, accurate alignment of very large numbers of sequences. *Methods Mol. Biol.* **2014**, *1079*, 105–116.
19. Saitou, N.; Nei, M. The neighbor-joining method: A new method for reconstructing phylogenetic trees. *Mol. Biol. Evol.* **1987**, *4*, 406–425.
20. Felsenstein, J. Evolutionary trees from DNA sequences: A maximum likelihood approach. *J. Mol. Evol.* **1981**, *17*, 368–376. [[CrossRef](#)]
21. Rzhetsky, A.; Nei, M. A simple method for estimating and testing minimum-evolution trees. *Mol. Biol. Evol.* **1992**, *9*, 945–967.
22. Kumar, S.; Stecher, G. Mega7: Molecular evolutionary genetics analysis version 7.0 for bigger datasets. *Mol. Biol. Evol.* **2016**, *33*, 1870–1874. [[CrossRef](#)] [[PubMed](#)]
23. Kimura, M.J. A simple method for estimating evolutionary rate of base substitution through comparative studies of nucleotide sequences. *J. Mol. Evol.* **1979**, *16*, 111–120. [[CrossRef](#)]
24. Felsenstein, J. Confidence limit on phylogenies: An approach using the bootstrap. *Evolution* **1985**, *39*, 783–791. [[CrossRef](#)] [[PubMed](#)]
25. Sambrook, J.; David, R. *Molecular Cloning: A Laboratory Manual*, 3rd ed.; Cold Spring Harbor Laboratory Press: Cold Spring Harbor, NY, USA, 2001.
26. Meier-Kolthoff, J.P.; Auch, A.F. Genome sequence-based species delimitation with confidence intervals and improved distance functions. *BMC Bioinform.* **2013**, *14*, 60. [[CrossRef](#)] [[PubMed](#)]
27. Yoon, S.H.; Ha, S.M. A large-scale evaluation of algorithms to calculate average nucleotide identity. *Antonie Van Leeuwenhoek* **2017**, *110*, 1281–1286. [[CrossRef](#)]
28. Avram, O.; Rapoport, D. MICR0B1aAL1Z3R—a user-friendly web server for the analysis of large-scale microbial genomics data. *Nucleic Acids Res.* **2019**, *47*, W88–W92. [[CrossRef](#)]
29. Alanjary, M.; Steinke, K. AutomlSt: An automated web server for generating multi-locus species trees highlighting natural product potential. *Nucleic Acids Res.* **2019**, *47*, W276–W282. [[CrossRef](#)]
30. Qin, Q.L.; Xie, B.B. A proposed genus boundary for the prokaryotes based on genomic insights. *J. Bacteriol.* **2014**, *196*, 2210–2215. [[CrossRef](#)]
31. Rodriguez-R, L.M.; Konstantinidis, K.T. Bypassing cultivation to identify bacterial species. *Microbe* **2014**, *9*, 111–118. [[CrossRef](#)]

32. Yarza, P.; Richter, M. The all-species living tree project: A 16s rRNA-based phylogenetic tree of all sequenced type strains. *Syst. Appl. Microbiol.* **2008**, *31*, 241–250. [[CrossRef](#)]
33. Richter, M.; Rosselló-Móra, R. Shifting the genomic gold standard for the prokaryotic species definition. *Proc. Natl. Acad. Sci. USA* **2009**, *106*, 19126–19131. [[CrossRef](#)] [[PubMed](#)]
34. Alikhan, N.F.; Petty, N.K. Blast ring image generator (BRIG): Simple prokaryote genome comparisons. *BMC Genom.* **2011**, *12*, 402. [[CrossRef](#)] [[PubMed](#)]
35. Ohta, H.; Hattori, R. *Sphingomonas oligophenolica* sp. nov., a halo- and organo-sensitive oligotrophic bacterium from paddy soil that degrades phenolic acids at low concentrations. *Int. J. Syst. Evol. Microbiol.* **2004**, *54*, 2185–2190. [[CrossRef](#)]
36. Blin, K.; Shaw, S. Antismash 6.0: Improving cluster detection and comparison capabilities. *Nucleic Acids Res.* **2021**, *49*, W29–W35. [[CrossRef](#)] [[PubMed](#)]
37. Li, S.; Shen, W. Darhd: A sequence database for aromatic ring-hydroxylating dioxygenase analysis and primer evaluation. *J. Hazard Mater.* **2022**, *436*, 129230. [[CrossRef](#)]
38. Nojiri, H.; Ashikawa, Y. Structure of the terminal oxygenase component of angular dioxygenase, carbazole 1,9a-dioxygenase. *J. Mol. Biol.* **2005**, *351*, 355–370.
39. Botelho, H.M.; Leal, S.S. Role of a novel disulfide bridge within the all-beta fold of soluble rieske proteins. *J. Biol. Inorg. Chem.* **2010**, *15*, 271–281. [[CrossRef](#)]
40. Brettin, T.; Davis, J.J. Rasttk: A modular and extensible implementation of the rast algorithm for building custom annotation pipelines and annotating batches of genomes. *Sci. Rep.* **2015**, *5*, 8365. [[CrossRef](#)]